

UNCLASSIFIED

**Defense Technical Information Center  
Compilation Part Notice**

**ADP013651**

**TITLE:** Evaluation of Time and Space Scales in a Spatially Developing 3D  
Turbulent Incompressible Mixing Layer by Using LES

**DISTRIBUTION:** Approved for public release, distribution unlimited

**This paper is part of the following report:**

**TITLE:** DNS/LES Progress and Challenges. Proceedings of the Third  
AFOSR International Conference on DNS/LES

**To order the complete compilation report, use: ADA412801**

The component part is provided here to allow users access to individually authored sections of proceedings, annals, symposia, etc. However, the component should be considered within the context of the overall compilation report and not as a stand-alone technical report.

The following component part numbers comprise the compilation report:

ADP013620 thru ADP013707

UNCLASSIFIED

# EVALUATION OF TIME AND SPACE SCALES IN A SPATIALLY DEVELOPING 3D TURBULENT INCOMPRESSIBLE MIXING LAYER BY USING LES

S. PELLERIN, A. DULIEU, C. TENAUD, L. TA PHUOC  
*L.I.M.S.I. - UPR CNRS 3251*  
*BP 133, F-91403 Orsay Cedex, France*

## Abstract

The spatial development of a 3D turbulent incompressible mixing layer is computed by using Large Eddy Simulation (LES). The time and space fluctuations of velocity components lead to the energy spectra. We can then to highlight the characteristic scales in both time and space. The energy spectra in time are in agreement with the turbulence theory and show two significant dimensionless frequencies; the largest one encountered for all the variables corresponds to the creation of main rolls. On the energy spectra in space, we can observe also two spanwise scales, one of them is found everywhere in the flow while the other one is representative of the phenomena inside the mixing zone.

**Key words:** Turbulence, Mixing layer, LES, Time and space scales.

## 1. Introduction

In incompressible flows, a mixing layer develops at the confluence of two parallel flows with different velocities, from the trailing edge of a flat plate (fig. 1.a). Instabilities then grow and eddy structures appear in the mixing zone, such as Kelvin-Helmoltz rolls, aligned with spanwise direction. A second instability creates other streamwise vortices (*braids*), observed between main structures. We study the spatial development of a 3D turbulent incompressible mixing layer, at a high turbulent Reynolds number. Therefore, control methods and flow reconstruction methods such as POD approach, require good unsteady descriptions of spatially developed flows.

The Reynolds number  $\mathcal{R}_e = 3.5 \times 10^4$  is based on the velocity difference  $U_{high} - U_{low}$  ( $U_{high} = 42.8$  m/s and  $U_{low} = 25.2$  m/s) and on the value of the

vorticity thickness experimentally measured at a reference section in the similarity zone, as  $\delta_\omega(x_0) = 0.03$  m.

The mixing layer development is computed with a LES code, using a velocity-vorticity formulation. The influence of the subgrid model has been previously studied (Lardat *et al.*, 1998). It was also pointed out that the upstream condition has a significant influence on the quality of the results (Pellerin *et al.*, 1999). The velocity and the Reynolds stress tensor profiles show self-similarity behavior and a good agreement with the reference experiment data (Delville, 1994).

Coherent structures have been visualized in this simulation and a study of the energy spectra in time and space, associated to this turbulent mixing layer computed by LES, would be able to find their time and space characteristics and are analyzed in order to recover the classic properties of the turbulence phenomena. Energy spectra are represented in appropriate  $y$  positions, to highlight the time and space characteristic scales of the flow. Our numerical results are compared to experimental ones and to the well known theoretical behaviors.

## 2. Numerical method : LES

We use a velocity-vorticity formulation of the Navier-Stokes equations. In LES, the exact field  $\phi$  is split into a filtered variable  $\bar{\phi}$  and a subgrid variable  $\phi'$ . The incompressible vorticity transport equation can then be written as:

$$\frac{\partial \bar{\omega}}{\partial t} - \nabla \times (\bar{v} \times \bar{\omega}) = -\frac{1}{\mathcal{R}_e} \nabla \times (1 + \nu_t) \nabla \times \bar{\omega} \quad ; \quad \bar{\omega} = \nabla \times \bar{v} \quad (1)$$

where  $\bar{v}$  and  $\bar{\omega}$  correspond to the filtered variables, resolved on the grid. The subgrid effects are based on the Taylor theory by means of a subgrid model using an eddy viscosity,  $\nu_t$ , related to the macroscopic quantities. The filtered velocity and pressure fields are obtained by a projection method (Lardat *et al.*, 1997).

A mixed scale subgrid model is used here (Ta Phuoc, 1994):

$$\nu_M = \left[ (C_S \Delta)^2 \|\omega\| \right]^\alpha \left[ C_B \Delta \sqrt{|k'|} \right]^{1-\alpha} \quad (2)$$

where  $k'$  corresponds to a kinetic energy associated to the subgrid cell. Note that we obtain classical vorticity and TKE models for special values of the  $\alpha$  exponent (0 and 1 respectively).  $C_S$  and  $C_B$  correspond to the Smagorinsky and the Bardina constants respectively. Following several simulations, we choose  $\alpha = 0.5$  which leads to the better results for this kind of problem. The advantage of this model is to dump smoothly the eddy viscosity in the regions where all the scales are well resolved.

The upstream condition corresponds to the mean velocities, according to experimental values (Delville, 1994). A rather high white noise is superimposed on this condition in order to obtain a correct development of the mixing layer (Pellerin *et al.*, 1999).

At the outlet surface, a convective transport hypothesis is applied (viscous effects neglected). The vorticity tangential components are calculated using an extrapolation along the characteristics. The outlet propagation velocity  $\bar{v}_x$  is deduced from vorticity, taking into account the mass flux conservation over this surface. In the inhomogeneous direction ( $y$ ), a slip condition is imposed at the lower and upper surfaces. A periodicity condition is used for the spanwise direction ( $z$ ).

A staggered M.A.C. grid is used for the spatial discretization (inhomogeneous grid in  $y$ ). Time and space derivatives are estimated by second order schemes. The LES code used has been vectorized and reaches very good performances, the use of FFT allowing speed improvement (for homogeneous directions). For example, on a NEC-SX5 with a maximal performance of 8 GFlops (IDRIS-CNRS, Orsay), we obtain for a classical run about 5 GFlops ( $7 \times 10^{-7}$  sec./time step/point).

### 3. Statistical study of the turbulent mixing layer

#### *Vorticity thickness, velocity and stress tensor components*

Solving unsteady Navier Stokes filtered equations for incompressible flows, we obtain then the unsteady velocity components. The figure 1.b shows the evolution in time (for 3000 time steps) of the flow direction component  $u$ , for three positions over the shear direction  $y$ . This variable has a strong turbulent behavior inside the mixing layer (at  $y = 0$  on the figure) and very low variations outside of it (at  $y = \pm \delta_\omega$  here).

Therefore, mean values are computed over a large integration time over 9000 time steps. Using a reference time of  $\delta_\omega(x_0)/(U_{high} - U_{low})$ , this interval corresponds to a dimensionless time of 61.7. We then obtain the mean velocity values and also the Reynolds stress tensor components. The mean values in time are next averaged over the transversal direction  $z$  to compare with experimental data.

The characteristic length of this flow is the vorticity thickness  $\delta_\omega(x)$  which increases linearly with the flow direction  $x$ . Turbulent structures in the mixing layer can be observed for  $y \in [-\frac{\delta_\omega}{2}, +\frac{\delta_\omega}{2}]$ , where  $y$  is the shear direction. The vorticity thickness is calculated from the mean longitudinal velocity  $\langle \bar{u} \rangle$ :

$$\delta_\omega(x) = [\langle \bar{u} \rangle_{max} - \langle \bar{u} \rangle_{min}] / \left( \frac{\partial \langle \bar{u} \rangle}{\partial y} \right)_{max} \quad (3)$$

The self similarity behavior is recovered when using the dimensionless parameters  $\delta_\omega$  and  $\Delta U = U_{high} - U_{low}$ . The velocity profiles show a good self-similarity behavior (fig. 2.a). While it is more difficult to converge the Reynolds stress tensor components, the resolved profiles are similar and show the quality of our simulation (fig. 2.b), using the mixing scale subgrid model and an appropriate upstream perturbation. All the results agree with experimental ones.

### *Energy spectra computation*

Energy spectra in time and space are computed from velocities, which can be stored through the calculation and on the 3D grid. There are about two million points in the mesh. Therefore, we select for storage five vertical positions  $y$ , such as the center of the mixing layer  $y = 0$ , its up and down boundaries  $y = \pm \delta_w/2$  and two positions outside of the mixing layer,  $y = \pm \delta_w$ . It is well known that these are the right positions to exhibit the characteristic scales. In addition, special values of the longitudinal  $x$  locations are selected inside the self-similarity zone, where the mixing layer is fully developed. In conclusion, the velocity storage is performed for all time steps and for all spanwise direction points, for these particular  $(x, y)$  locations (these positions are represented on figure 1.a).

The Kintchine's theorem about random steady functions (Chassaing, p46, 2000) allows to obtain the energy spectra using a Fourier transformation for velocity fluctuations. The energy spectra in time as functions of frequencies  $f$  are computed with a common vectorized FFT. The same procedure is followed in space, for the transversal direction  $z$ . The energy spectra in space are represented as function of the wave numbers  $k_z$ .

## 4. Energy spectra results and characteristic scales

For a normalized representation, we use the dimensionless wave numbers  $k_{za}(x) = k_z * \delta_w$  and the dimensionless frequencies  $f_a(x) = \frac{f \delta_w}{U_{ref}}$ . We choose for the reference velocity  $U_{conv} = (U_{high} + U_{low})/2$ , according to the Taylor's hypothesis. Energy spectra are then plotted as function of the (local) dimensionless frequencies  $f_a$  and the (local) dimensionless wave numbers  $k_{za}$ .

Some characteristic dimensionless frequencies or wave numbers can be identified and correspond to the characteristic scales in time and space. For time energy spectra, the characteristic scale is found for the maximal value, just before the theoretical fall down. Spatial evolutions are controlled by a spatial scale which is a wave length, obtained by  $\Lambda_z = 1/k_z$  and unsteady phenomena are characterized by a time scale  $T = 1/f$ .

Energy spectra in space, associated to the spanwise direction  $z$ , are presented on figure 3 for  $u_x$ ,  $u_y$  and  $u_z$  velocity components, as function of the dimensionless wave numbers. Spectra are plotted for two different  $x$  locations. For every  $y$  position in the mixing layer, we find equivalent evolutions for both  $x$  positions. Spectra have maximal values in the center of the mixing layer, at  $y = 0$  and decrease from the center to outside. Outside of the mixing zone, energy spectra present very small intensities. Therefore, energy is localized in the mixing layer where the velocity gradient is representative of the flow behavior.

A first characteristic spatial scale is encountered in energy spectra for all velocities. Its value is about 0.15-0.18 and coincides with the largest scale (wave length) observed experimentally, equal to 0.15. This scale is representative of turbulent

phenomena everywhere in the flow for  $u_y$  and  $u_z$  velocities (figs. 3.a and 3.b) and outside of the mixing layer for  $u_x$  (fig 3.a).

We find a second spatial scale in  $u_x$  energy spectra, which characterizes the spatial evolution inside the mixing layer. This scale is 0.5 at the boundaries of the shear zone ( $\pm \delta_\omega/2$ ) and stabilizes itself at 0.65 in  $y = 0$ . The  $u_y$  energy spectra show also this characteristic scale, because of divergence free effects. In these spectra, this scale is clearly visible only in the center of the mixing layer, at  $y = 0$ , and is equal to 0.7. This second scale has been estimated experimentally to be equal to 0.5.

Therefore, the characteristic spatial scales obtained numerically are in good agreement with experimental results, which means that the spatial behaviors must be rather well simulated. The main conclusion is the highlight of two characteristic scales for  $u_x$ , one representing phenomena inside the mixing layer and the other outside of the mixing zone.

The characteristic spatial scale representative of phenomena inside the mixing layer,  $kz_n = kz * \delta_\omega \simeq 0.5 - 0.65$ , can be associated to the wave length  $\Lambda_z \simeq [1.54 - 2.] \delta_\omega$ . This spanwise scale characterizes the spacing between two successive secondary structures (braids). We recover approximatively experimental results of Bernal and Roshko for the equivalent problem.

Figure 4.a represents the time energy spectra for  $u_x$  velocity, using as self-similarity parameter, the dimensionless frequency  $\frac{f \delta_\omega}{U_{conv}}$ . Inside the mixing layer, from the center  $y = 0$  to the frontiers  $y = \pm \delta_\omega/2$ , energy spectra have equivalent evolutions and are similar for the three different chosen positions  $x$ . A characteristic scale  $f_a$  less than 0.2 is clearly found and agrees with the experimental value of 0.15 observed by Delville (1995). An other time scale expresses the behavior outside the mixing layer. The value of this scale compares well quantitatively with the experimental one equal to 0.3.

Energy spectra for  $u_y$  is plotted on figure 4.b. Everywhere within the flow, for all  $y$  positions, the same scale is representative of turbulent phenomena, about 0.3. We don't represent here energy spectra for the transversal velocity  $u_z$  because we find the same behavior as  $u_y$ . In addition, these two velocities have energy spectra which do not depend on the  $x$  position.

The main characteristic time scale  $f_a \simeq 0.3$  can be associated to a longitudinal wave length  $\Lambda_x = T * U_{conv}$ , which controls longitudinal space evolutions. We can then write  $\Lambda_x = 3.33 \delta_\omega$ . This longitudinal length represents the spacing between two successive spanwise vertices (Kelvin-Helmoltz instabilities). If we consider the ratio between the transversal wave length  $\Lambda_z$  and the longitudinal one,  $\Lambda_z/\Lambda_x \simeq 0.46 - 0.6$  which compare quantitatively well with the experimental value of  $2/3$  usually found.

On figures 4.a and 4.b, the decrease of curves after their maximal values (characteristic scale in time), have at least over one decade a correct slope of approximatively  $-5/3$ , according to the well known theoretical slope of the energy cascade.

## 5. Conclusion

A 3D spatially developed mixing layer is studied numerically using LES. Energy spectra are computed in order to highlight the characteristic scales in both time and space. Two spanwise scales are found; one is encountered everywhere in the flow and the other is representative of the spanwise spacing between braids. In addition, two dimensionless frequencies are observed on energy spectra in time, which behave well. The largest frequency corresponds to Kelvin-Helmoltz instabilities.

## Acknowledgements

The authors would like to acknowledge J. Delville from C.E.A.T. of Poitiers, France, for his collaboration concerning his experimental results. The authors would also acknowledge the support of I.D.R.I.S.-C.N.R.S (Orsay, France), where the calculations have been performed on a NEC-SX5.

## References

- Bertagnolio, F. (1996) Thèse de Doctorat de l'Université Pierre et Marie Curie, Paris 6.
- Chassaing, P. (2000) *Turbulence en mécanique des fluides*, Cépaduès Editions, Toulouse.
- Delville, J. (1994) Characterization of the organization in shear layers via the proper orthogonal decomposition, *Applied Scientific Research*, **53**, pp. 263-281.
- Delville, J. (1995) *La décomposition orthogonale et l'analyse de l'organisation tridimensionnelle d'écoulements turbulents cisailés libres*, Thèse de Doctorat de l'Université Pierre et Marie Curie, Paris 6.
- Lardat, R. 1997 Thèse de Doctorat de l'Université d'Orsay, Paris 11.
- Lardat, R., Dulieu, A., Ta Phuoc, L. and Tenaud, C. (1998) L.E.S. of a spatially developing 3-D incompressible mixing layer with velocity-vorticity formulation, 16<sup>e</sup> *ICNMF*, Arcachon, France.
- Lardat, R., Bertagnolio, F. et Daube, O. (1997) La formulation vitesse-tourbillon en maillage décalé : une méthode de projection, *C.R.Ac.Sc.*, **324**, II b, pp. 747-753.
- Pellerin, S., Dulieu, A., Ta Phuoc, L. and Tenaud, C. (1999) Incompressible 3-D mixing layer using LES : Influences of subgrid scale models and of upstream perturbations, *ISCFD'99*, Bremen, Germany. Proceedings published in a Special Issue of *Computational Fluid Dynamics Journal*, **9**, no.1, April 2001.
- Ta Phuoc, L. (1994) Aérodynamique instationnaire turbulente - Aspects numériques et expérimentaux, *Journée Thématique DRET*, Paris, France.

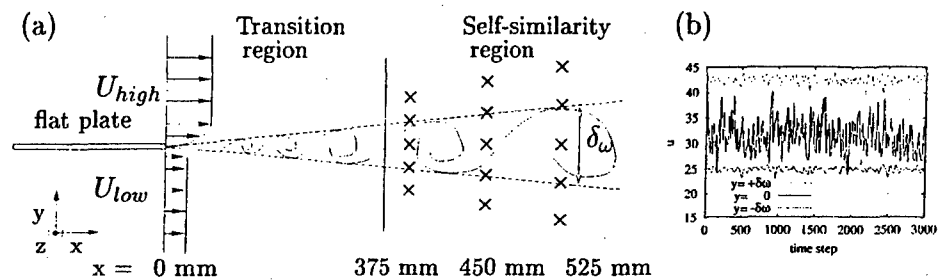


Figure 1. (a) Spatially developing mixing layer geometry. The mixing phenomena establishes behind the trailing edge of a flat plate, at the confluence of two different velocity turbulent flows;  $\times$  :  $(x, y)$  storage locations for energy spectra computation; (b) Longitudinal velocity  $u$  inside the mixing layer at  $y = 0$  and outside at  $y = +\delta_\omega$  ( $u \simeq U_{high} = 42.8$  m/s) and  $y = -\delta_\omega$  ( $u \simeq U_{low} = 25.2$  m/s), evolution for 3000 time steps.

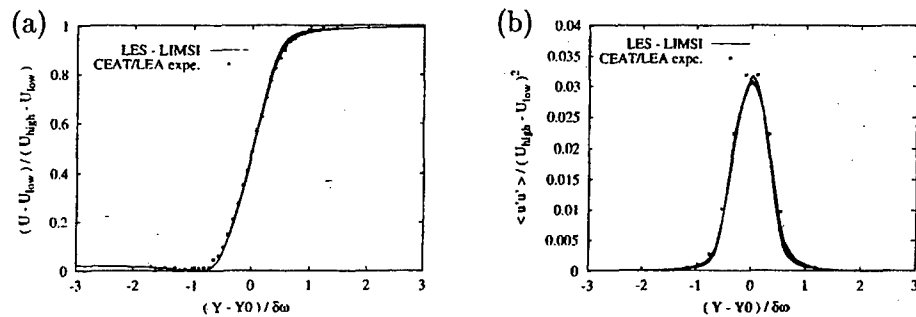


Figure 2. Superposition of profiles (at ten streamwise locations) versus the self-similarity parameter  $(y - y_0)/\delta_\omega$ . (a)  $u_x$  mean velocity; (b) first component of the Reynolds stress tensor,  $\langle \bar{u}^2 \rangle$ . L.E.S. performed using mixed scale model and white noise perturbation of 7.5%  $U_{high}$ .



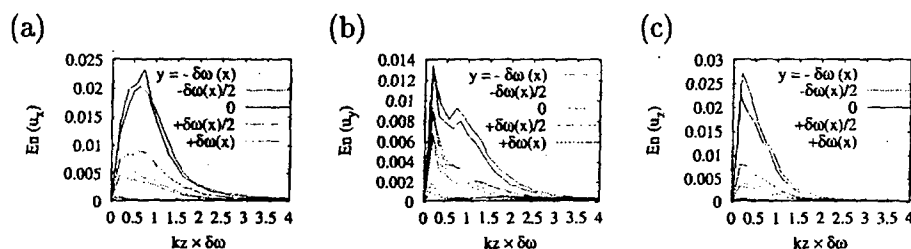


Figure 3. Spatial energy spectra for the spanwise direction  $z$ , inside and outside the mixing layer, for two  $x$  locations from the flat plate, 450 mm and 525 mm: (a) energy spectra for  $u_x$  velocity, which show two characteristic scales in space; (b) energy spectra for  $u_y$  velocity; (c) energy spectra for  $u_z$  velocity.

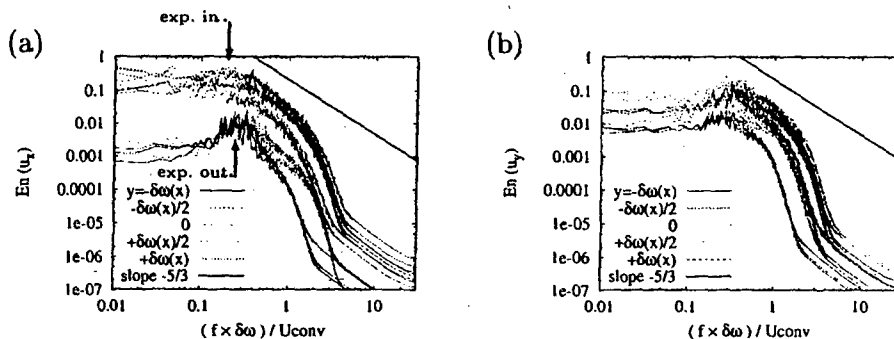


Figure 4. Time energy spectra inside and outside the mixing layer, for three  $x$  locations from the flat plate, 375 mm, 450 mm and 525 mm: (a) energy spectra for  $u_x$  velocity, which show two characteristic scales in time; (b) energy spectra for  $u_y$  velocity, with only one characteristic scale.